

# Design and control of a spherical mobile robot

J Alves and J Dias\*

Departamento de Engenharia Electrotécnica e de Computadores, Institute for Systems and Robotics, Universidade de Coimbra—Polo 2, Coimbra, Portugal

**Abstract:** This paper describes a type of mobile robot with a spherical shape designed to act as a platform to carry sensing devices or actuators in an environment where the conditions are harsh and the stability of the mechanical platform is critical. A remotely controlled internal unit drives the spherical robot. The paper focuses on the design and motion control of a robot with a spherical shape. The developed control modules are implemented in digital programmable logic devices, using a hardware description language named VHDL. The digital hardware controls multiple devices: a multichannel analogue-to-digital (A/D) converter, a pair of radio-frequency (RF) modules and four radio-controlled (R/C) servos. The robot motion is modelled by a configuration space function using the path curvature. The motion controller was designed to drive the robot to the desired path using control based on the path curvature. Because of the lack of a special steering mechanism, the robot steers only by controlling the displacement of its centre of gravity.

**Keywords:** spherical mobile robot, remotely controlled, control modules, VHDL, digital hardware

## NOTATION

$a$ or $\xi$	scalars
$a^{-1}$	inverse (the equivalent for the following)
$t$ or $\omega$	applied vectors (examples: translation vector and rotational vector)
$\{O\}$	coordinate frame (example: inertial coordinate system)
${}^R\mathbf{R}_D$	rotation matrix relating the orientation of referential $\{D\}$ relative to referential $\{R\}$
${}^D\mathbf{p}$	vector expressed in referential $\{D\}$ (example: vector with coordinates of a point)
${}^R\boldsymbol{\omega}_M$	vector expressed in referential $\{R\}$ (example: vector of angular velocity of the object $M$ )

## 1 INTRODUCTION

When developing mobile robots for uneven environments, typically encountered in missions outdoor, mobility is one of the central issues. Different mobile robots use legs, wheels, crawlers, or a combination of

these, for locomotion. However, there is a need to develop more efficient and versatile locomotion mechanisms adaptable to an uneven or bumpy path.

This paper presents a different mobile robot class that can achieve many kinds of unique motion, such as all-direction driving and motion on rough ground, without great loss of stability. The structure adopted for the robot presented in this paper is one of a spherical mobile robot, which can be seen in Fig. 1.



**Fig. 1** Prototype of the spherical robot

*This paper was presented at the International Conference on 'Mechatronics 2003' (ICOM 2003) held at Loughborough University, Leicestershire, UK on 18–20 June 2003. The MS was received on 7 April 2003 and was accepted after revision for publication on 22 July 2003.*

\* Corresponding author: Departamento de Engenharia Electrotécnica e de Computadores, Institute for Systems and Robotics, Universidade de Coimbra—Polo 2, 3020-290 Coimbra, Portugal.

A few other authors have developed similar work with spherical mobile robots, but most of them are still in the stage of perfecting their systems. Bhattacharya and Agrawal [1] use the principle of angular momentum conservation. This robot uses two mutually perpendicular rotors placed inside the spherical shell, causing the shell to rotate in response to their own rotation. The robot proved to be accurate in following a trajectory in a plane.

A different motion generation approach is to cause an unbalance in the robot by displacing its gravity centre; in turn, the gravitational force causes the robot to rotate in order to restore its equilibrium. Halme *et al.* [2, 3] propose a robot with a single wheel resting on the bottom of the spherical shell. This construction proved to be well suited for obstacle crossing and moving in rough terrain.

Koshiyama and Yamafuji [4] presented a robot that included two internal pendulums used for displacing the robot's gravity centre. The robot was able to run over obstacles at high-speed, maintaining a great stability. However, it was not able to move in all directions at all times since it had an external support sticking out from the spherical cover for the purpose of carrying small objects.

The motion control and feedback stabilization of a spherical mobile robot refers to the task of rolling a sphere to fulfil a desired path without slipping on a horizontal surface—the plate-ball problem. The kinematics model of the rolling sphere cannot be reduced to a chained form and the non-holonomic control and motion planning algorithms are not applicable [5]. However, the plate-ball system is controllable, as presented in reference [6], and the same holds for two rolling spheres if their radius is different. The control of plate-ball systems, which is a classical problem in rational mechanics, was studied in reference [7]. An optimal solution for the plate-ball problem was proposed in reference [8], which minimizes the length of the curve traced out by the sphere on the fixed plane and the integral of the kinetic energy along the path.

This paper focalizes on the robot modelling, design and motion control based on the path curvature. In section 5, a feedback law for stabilizing a rolling sphere along a predefined path is presented. A control algorithm that utilizes two control actions that are applied alternately was presented in reference [9]. In this paper, an approach using just one control action is used. The motion controller was designed to control the robot continuously on the desired path using control based on the path curvature. The robot steers by controlling the displacement of its centre of gravity. The experimental results show the feasibility and robustness of the method.

This paper also focuses on the electronics used in the robot. In recent years, new technologies for programmable logic devices (PLDs) and practical hardware description languages (HDLs) have been developed. This hardware solution has the advantages of speed and

parallelism over the software solution, and allows a similar degree of flexibility. In this work, the adopted HDL for description of the hardware function was the IEEE Standard VHDL, for which there are many available tutorials (see, for example, reference [10]).

The topics described in the article are the following. In section 2, the mechanical structure for the spherical robot is presented and how the robot's motion is generated. A generic kinematical and dynamical model is obtained in section 3. Section 4 is devoted to the robot's construction and instrumentation. In section 5, the focus is on control and section 6 shows some of the results obtained. Conclusions and a discussion on how to address other research topics based on this robotic platform are described in section 7.

## 2 THE SPHERICAL ROBOT

The mobile robot presented in this paper has an external spherical shape. It consists of a spherical capsule with an internal unit that causes the robot to roll, therefore inducing motion in the robot. The spherical capsule is made of transparent plastics in order to allow visibility from inside the sphere to outside. A radio link allows the exchange of information between the internal unit and the external control unit.

One of the most important decisions made during the designing process of this spherical robot concerns the type of internal unit used to induce motion. Different options can be used and since the principle of angular momentum conservation is not well suited for irregular terrain, where unexpected external momentums can easily appear, the solution adopted for this paper was similar to the one from reference [2]. Instead of using an internal vehicle with just one wheel, an assembly with a small four-wheeled vehicle was adopted as the internal unit. Since each wheel can be controlled separately it is possible to generate different motion curves.

The projected internal unit can be seen in Fig. 2. Its high symmetry is intentional and tries to prevent kinematical and dynamical modelling errors caused by the possible turning over of the unit inside the spherical shell. The symmetry of the vertical axis also makes the robot have its support base levelled when at rest.

Figure 3 illustrates the side and front view model of the robot respectively. These views are used to define two planes for modelling the robot dynamics. For each plane, a dynamic model is defined, all of which have equivalent dynamic characteristics. By combining the spherical geometry of the robot with a differential drive configuration for the internal unit the robot achieves very interesting motion properties that allow it to behave like a holonomic robot.

In order for the spherical robot to move in a predetermined way, a control unit is needed. The robot will move if the centre of gravity of the internal unit changes its

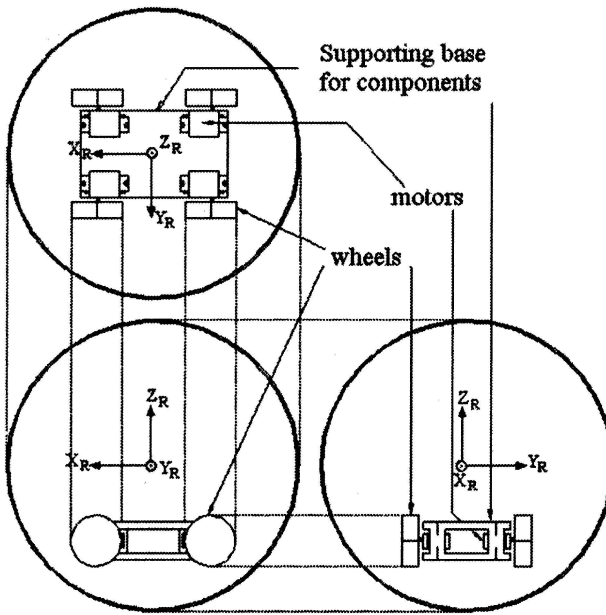


Fig. 2 Structure of the internal unit

position from rest or an equilibrium position. The robot moves in a straight line if, as illustrated in Fig. 3a, the angle  $\beta \neq 0$ . To steer the robot the lateral position of the centre of mass must be changed, as illustrated in Fig. 3b. The steering is controlled by the angle  $\xi$ , which is responsible for lateral displacement of the centre of gravity. The robot trajectories are equivalent to paths that can be defined in the ground plane. The path projected on the ground, as illustrated in Fig. 4, is used to design the steering control law presented in section 5. The robot changes its motion direction by controlling the position of the centre of gravity of the internal unit inside the sphere. In the following section, a kinematical and dynamical model of the robotic system is described.

### 3 MOTION MODEL

A basic motion analysis for the spherical robot can be easily performed using techniques similar to other fields of robotics and explained in many textbooks, such as, for example, references [11] and [12]. In the following paragraphs, the kinematics of this device will be developed.

Consider the contact point  $c = (x_c, y_c)$  between the spherical robot and the plane, as shown in Fig. 5. Assume that there are no slippages between the spherical shell and the plane of movement. This point  $c$  moves and describes a continuous trajectory in the plane when the spherical robot rolls. An inertial coordinate frame  $\{O\}$  is attached to the planar surface and another coordinate frame  $\{C\}$  is attached to the instantaneous contact point  $a$  between the sphere and the plane. In respect to coordinate frame  $\{O\}$ , the motion of coordinate frame  $\{C\}$  consists only of a linear motion along its  $x$  axis and a rotational motion around the  $z$  axis. Since the only component of velocity  $v$  in coordinate frame  $\{C\}$  is along the  $x$  axis, the motion equations on the plane can be written as

$$x_c(t) = x(0) + \int_0^t v(t) \cos(\alpha_1) dt \quad (1)$$

$$y_c(t) = y(0) + \int_0^t v(t) \sin(\alpha_1) dt \quad (2)$$

$$\alpha_1 = \alpha_1(0) + \int_0^t \omega_c(t) dt \quad (3)$$

#### 3.1 Kinematical model

Inside the spherical robot, consider the more general case of the internal unit being a single virtual wheel. This

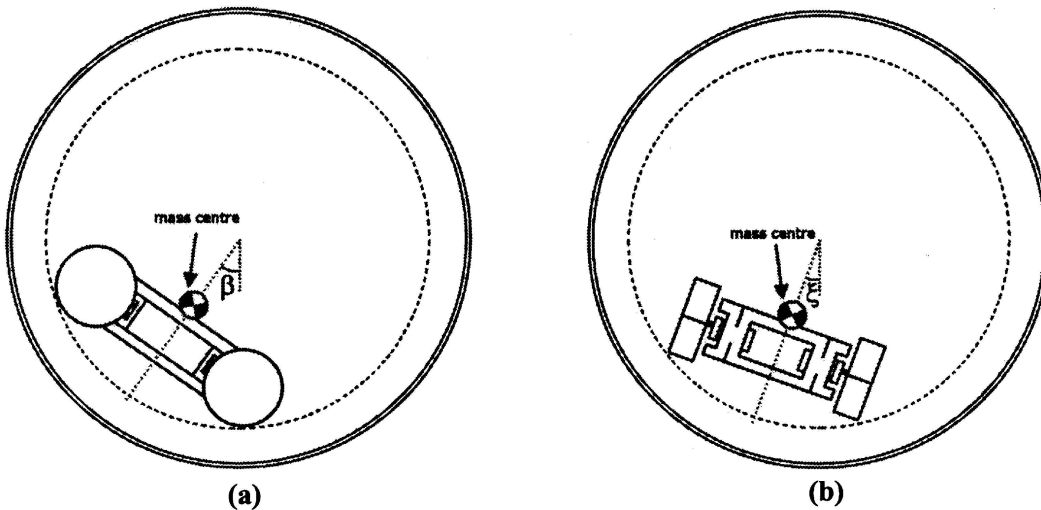
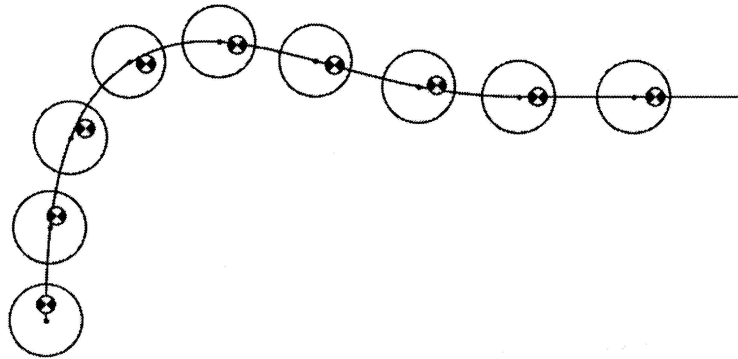
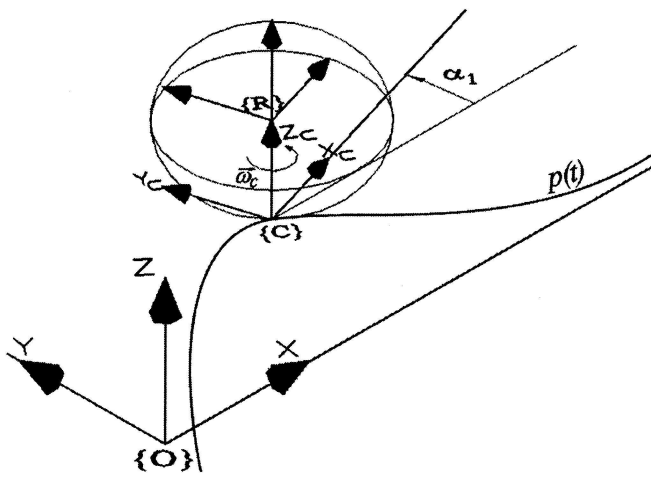


Fig. 3 Motion model is equivalent to a pendulum: (a) side view, (b) front view



**Fig. 4** Centre of gravity of the robot projected on the ground. Robot steering is controlled based on the path curvature  $k(t)$



**Fig. 5** Motion on a plane

virtual wheel rests in a spherical shell with its internal radius equal to the radius of the circle described by the contact points between the internal unit's wheels and the inner spherical surface of the real robot.

As seen in Fig. 6, a coordinate frame,  $\{R\}$ , is attached to the centre of the sphere. Another coordinate frame,  $\{D\}$ , is attached to the centre of the virtual wheel with the  $x$  axis having the wheel's orientation and the  $y$  axis being perpendicular to it. An auxiliary coordinate frame,  $\{T\}$ , is attached to the robot's mass centre.

The virtual wheel has radius  $r_w$  and rotates with an angular velocity  $\omega_M$  around the  $y$  axis of coordinate frame  $\{D\}$ . This angular velocity  $\omega_M$  translates into a linear velocity,  $v_1$ , for the contact point between the virtual wheel and the inner spherical surface. The virtual wheel also presents angular velocity  $\dot{\gamma}$  around the  $z$  axis of coordinate frame  $\{D\}$  in order to reorient the direction of motion.

The rotation speed of the wheel, with respect to coordinate frame  $\{D\}$ , is given by

$${}^D\boldsymbol{\omega}_M = \begin{bmatrix} 0 & v_1/r_w & 0 \end{bmatrix}^T \quad (4)$$

Defining  ${}^R\mathbf{R}_D$  as a rotation matrix that expresses the

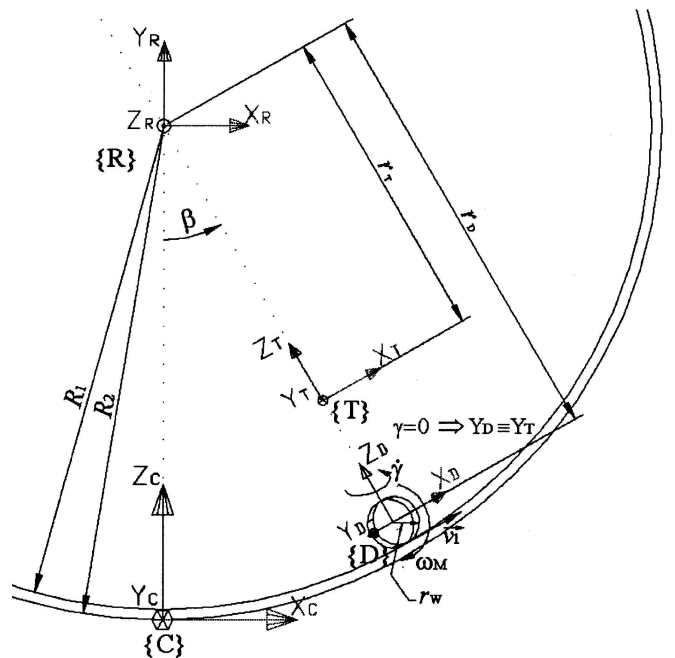


**Fig. 6** Motion inside the spherical robot

orientation of the referential  $\{D\}$  with respect to  $\{R\}$ , this rotation speed [equation (4)] can be expressed in coordinate frame  $\{R\}$  as

$${}^R\boldsymbol{\omega}_M = {}^R\mathbf{R}_D {}^D\boldsymbol{\omega}_M = -\frac{v_1}{r_w} \begin{bmatrix} c_\beta s_\gamma \\ s_\beta s_\gamma \\ c_\gamma \end{bmatrix} \quad (5)$$

where  $c_\theta$  and  $s_\theta$  are shorthand for  $\cos(\theta)$  and  $\sin(\theta)$ .

The virtual wheel angular velocity  ${}^R\boldsymbol{\omega}_1$  can be decoupled on two velocities,  ${}^R\boldsymbol{\omega}_{1M}$  and  ${}^R\boldsymbol{\omega}_{1y}$ , resulting from velocities  $\omega_M$  and  $\dot{\gamma}$  (see Fig. 6). As illustrated in Fig. 7, these two velocities are related by the equation

$${}^R\boldsymbol{\omega}_1 = {}^R\boldsymbol{\omega}_{1y} + {}^R\boldsymbol{\omega}_{1M}$$

From equation (5), and considering the total radius inside the sphere ( $r_D + r_w$ ), the velocity component  ${}^R\boldsymbol{\omega}_{1M}$

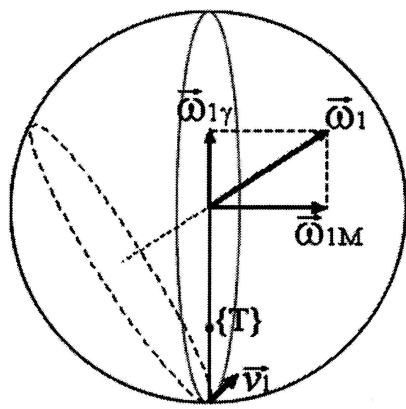


Fig. 7 Representation of the internal unit's angular velocity

is given by

$$\begin{aligned} {}^R\boldsymbol{\omega}_{1M} &= \frac{r_w}{r_d + r_w} (-{}^R\boldsymbol{\omega}_M) \\ &= \frac{v_1}{r_d + r_w} \begin{bmatrix} c_\beta s_\gamma \\ s_\beta s_\gamma \\ c_\gamma \end{bmatrix} \end{aligned} \quad (6)$$

which expresses its proportionality to  ${}^R\boldsymbol{\omega}_M$ . Defining  ${}^R\mathbf{R}_T$  as a rotation matrix that expresses the orientation of the referential  $\{T\}$  with respect to the referential  $\{R\}$ , and expressing velocity  $\dot{\gamma}$  as a vector, the component  ${}^R\boldsymbol{\omega}_{1\gamma}$  is given by

$$\begin{aligned} {}^R\boldsymbol{\omega}_{1\gamma} &= {}^R\mathbf{R}_T {}^T\dot{\gamma} = {}^R\mathbf{R}_T \begin{bmatrix} 0 \\ 0 \\ \dot{\gamma} \end{bmatrix} \\ &= \begin{bmatrix} -\dot{\gamma}s_\beta \\ \dot{\gamma}c_\beta \\ 0 \end{bmatrix} \end{aligned} \quad (7)$$

It should be noticed that only the two components of  ${}^R\boldsymbol{\omega}_1$  along the  $z$  axis and the  $y$  axis are important for this modelling, which can be expressed by algebraic transformations

$$\dot{\beta} = ({}^R\boldsymbol{\omega}_1)^T \begin{bmatrix} 0 \\ 0 \\ 1 \end{bmatrix} = \frac{v_1 c_\gamma}{r_d + r_w} \quad (8)$$

$$\dot{\alpha}_1 = ({}^R\boldsymbol{\omega}_1)^T \begin{bmatrix} 0 \\ 1 \\ 0 \end{bmatrix} = \frac{v_1 s_\beta s_\gamma}{r_d + r_w} + \dot{\gamma} c_\beta \quad (9)$$

The linear velocity of the robot is then expressed by

$$v = \dot{\beta} R_2 \quad (10)$$

Results from equations (8), (9) and (10) can be combined with equations (1), (2) and (3), giving the global kinematical model of the spherical robot.

### 3.2 Dynamic model

The dynamic model is necessary to model the robot's behaviour and to have a good knowledge of its motion properties. Since the robot has its own inertia, it will not respond instantly to velocity commands.

Assume, without loss of generality, that the internal unit concentrates its mass  $M$  in a single point, which is the origin of referential  $\{T\}$  (see Fig. 8). Define a plane passing through the origins of the referentials  $\{R\}$ ,  $\{T\}$  and  $\{C\}$ . This plane will be used as the reference plane in order to develop the dynamic model below. To simplify the description referential names will be omitted.

The unbalanced mass centre translates into a torque given by the expression

$$\tau = d_{CM} \times Mg \quad (11)$$

This torque causes an angular acceleration as given by

$$\tau = I\alpha' \quad (12)$$

Combining equations (11) and (12), the angular acceleration  $\alpha'$  can be expressed as a function of the angle  $\theta$  as

$$d_{CM} Mg \sin(\theta) = I\alpha' \quad (13)$$

since  $s_\theta$  and  $s_\beta$  are related by trigonometric relations

$$\frac{r_T}{s_\theta} = \frac{d_{CM}}{s_\beta} \Leftrightarrow s_\theta = \frac{s_\beta r_T}{d_{CM}} \quad (14)$$

and, since angle  $\beta$  is easier to obtain from sensory data, expression (13) is rewritten as a function of  $\beta$  instead of  $\theta$ :

$$r_T M g s_\beta = I\alpha' \quad (15)$$

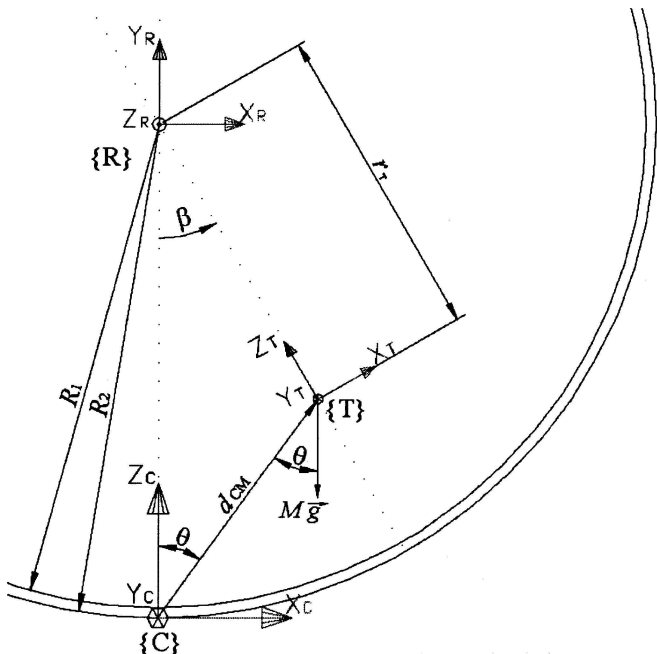


Fig. 8 Effect of moving the internal unit

In this implementation, the angle  $\beta$  is obtained from inertial sensors, as described in the next section.

The linear acceleration of the spherical robot can easily be determined since it is related to its angular acceleration through the expression

$$a' = \alpha' R_2 \quad (16)$$

It is then possible to express the linear acceleration of the spherical robot as a function of  $\beta$ , using the equation

$$a' = \frac{r_T M g s_\beta}{I} R_2 \quad (17)$$

It should be noticed that the acceleration of the spherical robot characterizes its motion dynamics in the plane passing through the origins of the referentials  $\{R\}$ ,  $\{T\}$  and  $\{C\}$ . It should also be noticed that the robot's moment of inertia,  $I$ , is not a constant in this case since the mass distribution of the robot around the contact point changes with rotation around that point. Therefore, the moment of inertia is a variable depending on angle  $\beta$ . This illustrates the difficulties of controlling this system using the dynamics model. In section 5 a control law using a configuration space based on the path curvature will be described.

#### 4 THE ROBOT'S CONSTRUCTION

In order to operate the robot and perform its control, a set of electronic equipment was designed and implemented. The actuators of the inertial unit are radio-controlled (R/C) servos modified for continuous rotation. This solution was adopted since they have high torque for their size and are easily available.

For motion control, inertial sensing was adopted as the feedback. The feedback was implemented in the robot by a basic navigation unit consisting of a three-axis accelerometer and a three-axis rate gyro. The gyros give heading information that is combined with the accelerometer data to determine the robot's acceleration, velocity and position relative to an inertial frame attached to a fixed point on the ground.

All of the control implemented in the robot was done in digital PLDs. Since the sensors used had analogue outputs, their interface with the PLDs was done through an analogue-to-digital (A/D) converter. As a way of simplifying the hardware in the robot, the motion control algorithms were implemented remotely on a computer, being the communication between the robot and computer based on radio-frequency (RF) transmitters and receivers.

##### 4.1 Calibration of the spherical shell

The controller assumes that the mass centre of the spherical shell is located at its geometric centre. To achieve this it is necessary to calibrate the spherical shell.

The spherical shell of this robot is composed of two similar halves. Since none of these halves have a homogeneous surface they behaved as shown in Fig. 9, when placed in a horizontal plane.

The procedure followed to calibrate the spherical shell consisted in increasingly placing small weights near point A, until angle  $\varepsilon$  came to zero. Applying this procedure iteratively to both halves on two orthogonal directions, the necessary steps were made to calibrate the spherical shell. This very practical procedure places the spherical robot's mass centre coincident to its geometric centre.

##### 4.2 Robot's control hardware

As mentioned above, the control algorithms were implemented in a remote computer, with communication through RF transmitters and receivers. In order to achieve full duplex, high-speed communication, a transmitter-receiver pair was used for communication in one direction and another pair for communication in the other direction. Figure 10 illustrates the interface between the computer and robot.

On the robot's side, all hardware interface and control was achieved using only PLDs. This decision provides true parallelism in the execution of several tasks, and allows high integration of circuits. A block diagram of the robot's architecture is illustrated in Fig. 11.

The 'Transmitter' and 'Receiver' circuits interact with the RF modules, respectively sending and receiving the data as they are used in the physical layer of communication. The RF modules only modulate/demodulate the bits to/from the RF spectrum, leaving all the data processing to the 'Transmitter'/ 'Receiver' circuits, which were designed using VHDL.

The data received by the robot are the desired speeds for each of the internal units' wheels. The circuit 'Servos Command' converts these desired speeds into command signals for controlling the rotation speed of the servos.

The circuit 'Read Sensors' interacts with an eight-channel analogue-to-digital converter (ADC) using the SPI interface protocol as described in its dataset [13]. The accelerometer and gyro outputs are connected to different ADC channels and the 'Read Sensors' circuit sequentially and continuously instructs the ADC to convert them all, feeding them back to the circuit 'Average'.

The circuit 'Average' serves mainly for sampling the

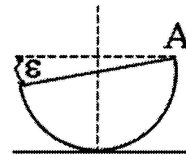


**Fig. 9** The spherical shell is divided in two and each half sphere is calibrated by levelling the great circle of the shell

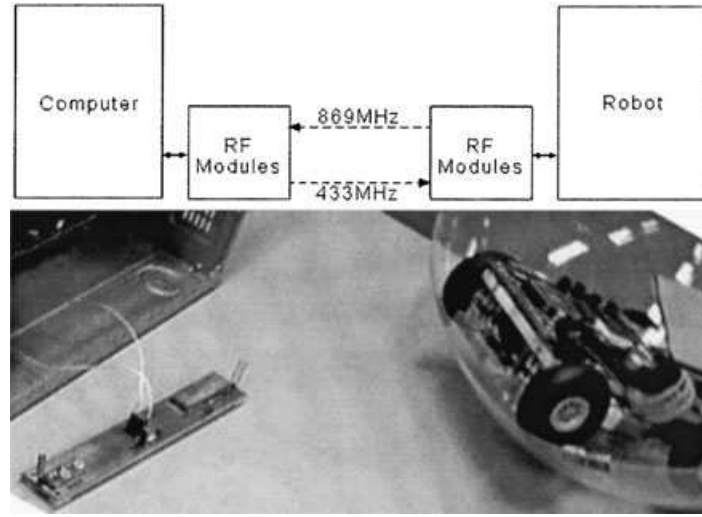


Fig. 10 Interface between the computer and robot

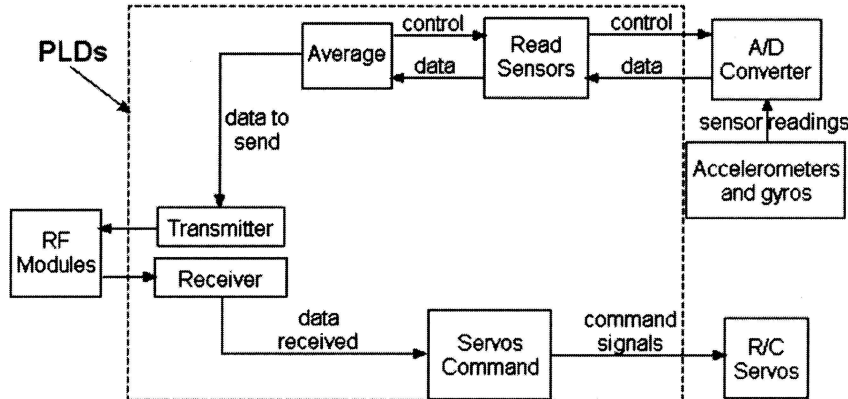


Fig. 11 Robot's architecture

sensors data at a higher rate than the one at which it is possible to transmit the data to the remote computer. To prevent losing important data from the sensors, these are sampled at a high rate and averaged during a certain period. This average is transmitted to the computer. In this way, high-frequency data can be included in the measurements transmitted to the computer. On the computer side, a data-acquisition board is used to interface with the RF modules and an interrupt service routine provides the interface between the control application and the data-acquisition board.

## 5 CONTROL

Consider the projection of the robot's centre of mass according to the surface's normal, as illustrated in Fig. 4. That position is the contact point  $c$  on the surface. Let  $(x_c, y_c)$  be the coordinates of the contact point  $c$  on this locus. The velocity constraints of the contact point

coordinates are

$$\begin{bmatrix} \dot{x}_c \\ \dot{y}_c \end{bmatrix} = \begin{bmatrix} v \cos \alpha_1 \\ v \sin \alpha_1 \end{bmatrix} \quad (18)$$

where  $v$  is the contact point velocity. That velocity can be related, as illustrated in Fig. 12, with the angular velocity  $\omega$  measured in the inertial coordinate frame  $\{O\}$  and the instantaneous radius of curvature  $r$  with centre in  $o$ . This velocity is given by the expression

$$v = r\omega \quad (19)$$

It should be noticed that equation (18) is the same as the rolling constraints of a typical mobile robot.

The status of the contact point  $c$  of the robot is described by a vehicle configuration, expressed by

$$q = (p, \alpha_1, k) = ((x_c, y_c), \alpha_1, k) \quad (20)$$

where  $p$  and  $\alpha_1$  denote its position and orientation respectively in the coordinate frame  $\{C\}$  and  $k$  is the path curvature in the inertial Cartesian coordinate

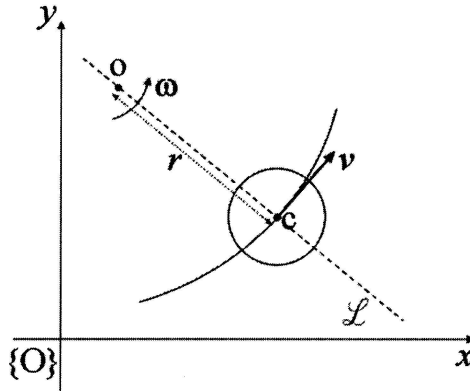


Fig. 12 Constraint in robot motion in the plan of movement

system. This description follows the description in reference [14], which is suitable for establishing a steering control law based on the curvature [14, 15].

All the variables in equation (20) are functions of time and path characteristics. The path curvature  $k$  is included in the vehicle configuration because it is assumed that the vehicle can execute a path that has curvature continuity.

If the curvature of the path is continuous, the robot's motion can be described as follows: define a line  $L$  fixed on the vehicle so that there is a rotational centre  $o$  on  $L$  with a rotational speed of  $\omega$  (Fig. 12). The contact point  $c$  is defined in  $L$  and defined as a vehicle reference point. Since the position of  $o$  is specified by the distance  $r$  from  $\{C\}$ , an instantaneous motion is described by only two variables  $(r, \omega)$  [or equivalently by  $(r, v)$ ] where  $v$  is the linear speed at the coordinate frame  $\{C\}$ . These control inputs can be replaced by the curvature  $k$  and the velocity  $v$  on the contact point, since the motion of the contact point  $c$  assumes the path curvature continuity. The curvature  $k$  can be expressed as

$$k = \frac{da_1}{ds} = \frac{1}{r} \quad (21)$$

where  $r$  and  $s$  are the instantaneous radius of the curvature from the centre of rotation  $o$  to the contact point  $c$  and the path length respectively. If the centre  $o$  of the rotation is at infinity, the robot will move on a straight path and the curvature and steering velocity will be zero. From equation (21), the robot's path curvature  $k$  can be controlled by controlling the steering velocity along the path. This robot configuration is illustrated in Fig. 13, where  $\alpha_1$  is measured about the  $x$  axis from the frame  $\{O\}$ .

The path curvature is a good variable to describe vehicle motions because  $k$  is more directly related to vehicle control and the curvature is independent of how the inertial coordinate system is placed. If the derivative of the curvature  $k$  is computed,

$$\eta = \frac{dk}{ds} \quad (22)$$

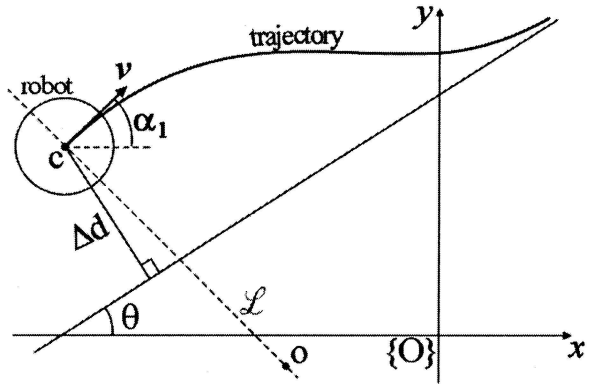


Fig. 13 Principle of path tracking

the constraint of a continuous curvature will be considered if the magnitude  $|\eta|$  is finite. Therefore, based on reference [14], the derivative of the path curvature is considered as fundamental for path tracking control and is expressed by the following control rule:

$$\frac{dk}{ds} = -Ak - B(\alpha_1 - \theta) - C \Delta d \quad \text{with } A, B, C \in \mathbb{R} \quad (23)$$

with respect to the path length  $s$ .

The variables  $\theta$  and  $\Delta d$  are the duration of the desired path line and the shortest distance between the robot and the desired path line respectively. The letters  $A$ ,  $B$  and  $C$  are constants used on this steering control function [14]. The term  $-Ak$  is a damping factor for the curvature, the term  $-B(\alpha_1 - \theta)$  is a feedback term for the angle error and the term  $-C \Delta d$  is a feedback term for the positional error.

## 6 EXPERIMENTAL RESULTS

The experiments with the spherical robot prototype validate the previous models. The robot shown in Fig. 1, was designed based on the models presented in section 3 and using the architectures and hardware described in section 4. The internal unit operates as a differential drive to give the robot the ability to turn in place, but although the construction with the four wheels is appropriate for driving in a straight line, when it comes to turning, there is some slipping of the internal unit inside the spherical shell. However, the closed-loop control, based on inertial sensing, copes with this situation without difficulty.

Figure 14 shows the robot reaction to step impulse applied to the internal unit, in this case the inclination angle. In this experiment, the robot is stopped and only the internal unit moves inside the spherical shell.

Figure 15 shows the robot reaction to a step input for the angle of inclination and for the robot's orientation. On these experiments, the robot is moving freely. Since there is an error in orientation, the robot first starts to

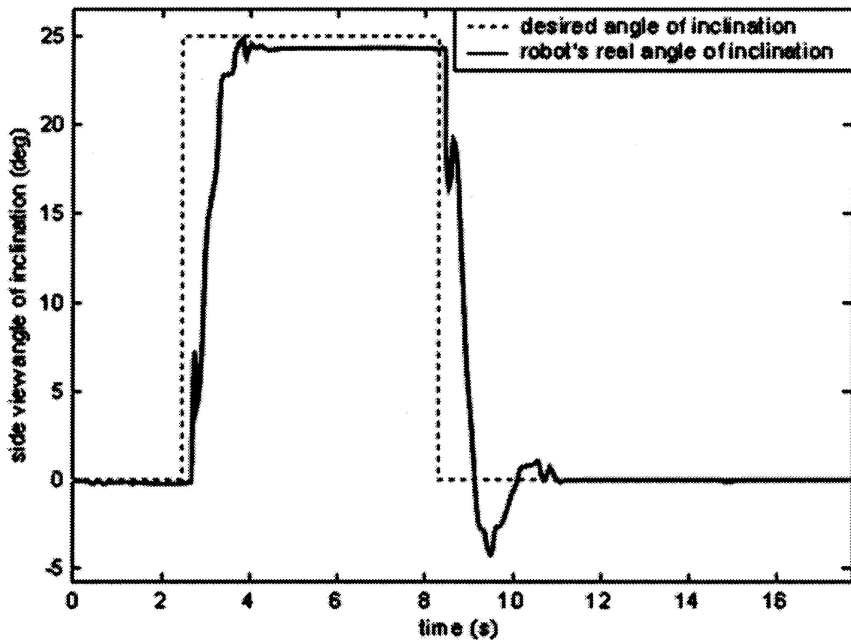


**Fig. 14** Response to step impulse applied to the inclination angle. The robot is forced to be stopped and only the internal unit moves inside the spherical shell

reorient itself to the desired orientation and, only after that, the desired angle of inclination is achieved. Since the robot is moving freely, it needs to keep the motors running in order to maintain an angle of inclination different from zero.

The experiments show that the robot can be driven easily in straight paths or paths with small curvature. The experiments also show that the control is more unstable for paths with a bigger curvature, but during them it was found that by using an internal unit with more mass the filters could be tuned to cope with the instabilities generated on the inertial sensors. Since the paths with big curvature are severe cases for these experiments, these adaptations will be the future improvements on the internal unit.

## 7 DISCUSSION AND CONCLUSIONS

This paper described the architecture, implementation and control of a mobile robot with a spherical shape. This robot was designed to act as a platform to carry sensing devices or actuators in an environment where the conditions are harsh or the stability of the mechanical platform is critical. When developing mobile robots for uneven environments, typically encountered in missions outdoor or in space, mobility is one of the central issues. Different mobile robots use legs, wheels, crawlers, or their combination, for locomotion. However, these systems need efficient and versatile locomotion mechanisms in order to adapt in uneven or bumpy paths. This mobile robot can achieve many kinds of unique motion,

such as all-direction driving and motion on rough ground, without great loss of stability.

The motion properties of the spherical mobile robot were analysed and verified by a set of experiments. The control of the robot's devices was built using digital programmable logic devices, which proved to be a very suitable solution for interconnection of devices achieving high integration of circuits in a mobile robot such as this.

One of the weakest properties of this particular robot's implementation is the plastic material used to produce the spherical shell surface. This material exhibits low friction between the robot and the ground on the contact point. In experiments with planar surfaces with low friction it was observed that it is not only the internal unit that turns inside the spherical shell but often the entire robot also turns in the opposite direction. A solution is to choose another surface shell coating and also to develop closed-loop control algorithms using the feedback from internal sensors to determine the real angle turned by the robot.

The development of other non-holonomic control algorithms using this platform is an interesting subject to address. The non-holonomic systems arise in finite dimensional mechanical systems where constraints are imposed on the motion that are not integrable [16]. This type of mobile platform is an interesting device used to develop new techniques for non-holonomic motion planning.

## ACKNOWLEDGEMENTS

The authors wish to thank the anonymous reviewers by their comments. They were very useful to improve the

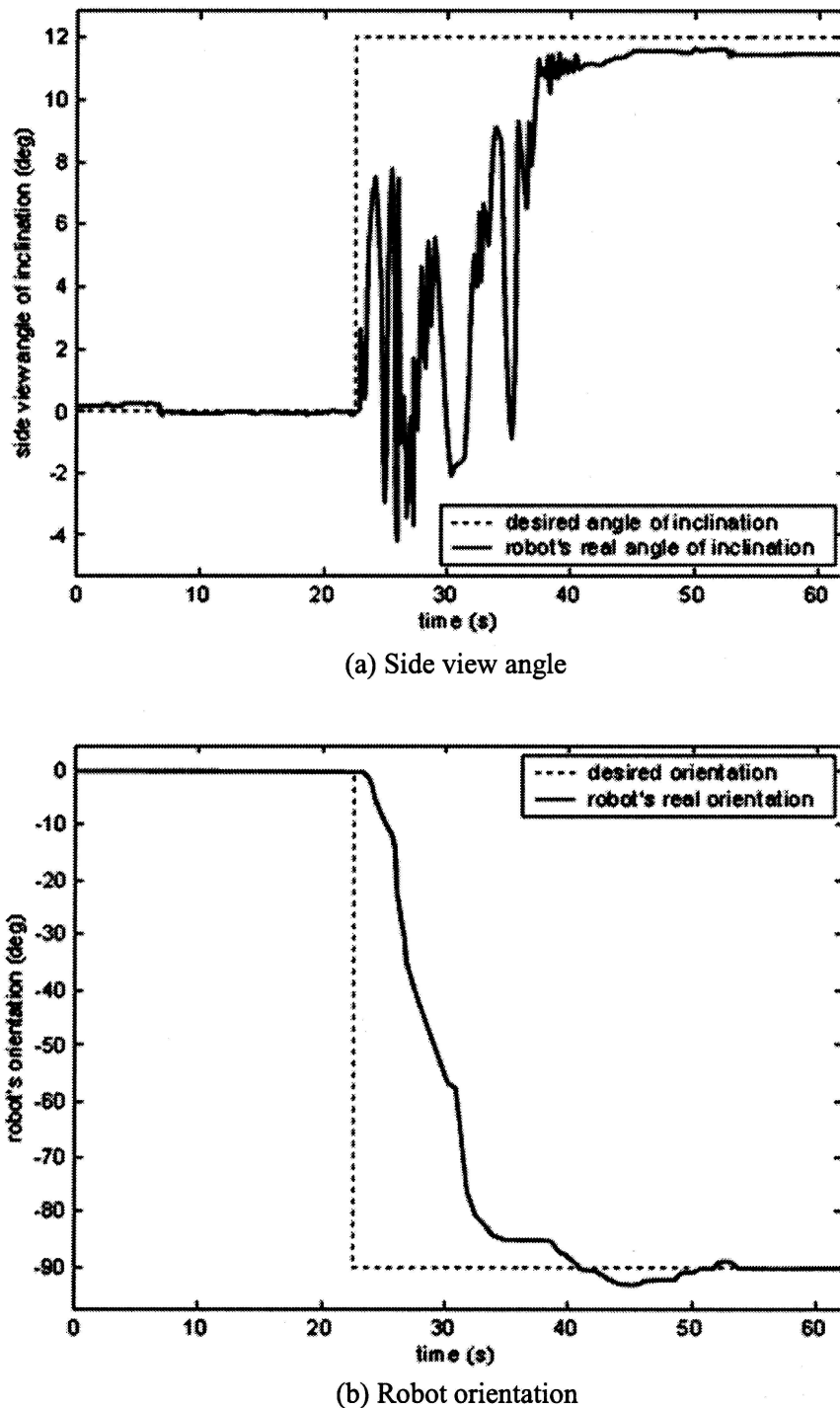


**Fig. 15** Response to the step impulse when the robot is moving freely. A step input is applied to both (a) the angle of inclination and (b) the robot's orientation

article and harmonize the entire notation throughout the article. This work has been supported by the Institute of Systems and Robotics at the University of Coimbra.

## REFERENCES

- 1 Bhattacharya, S. and Agrawal, S. K. Design, experiments and motion planning of a spherical rolling robot. In Proc. Instn Mech. Engrs Vol. 217 Part I: J. Systems and Control Engineering

Proceedings of the IEEE International Conference on *Robotics and Automation*, San Francisco, California, April 2000, pp. 1207–1212.

- 2 Halme, A., Suomela, J., Schönberg, T. and Wang, Y. A spherical mobile micro-robot for scientific applications. Technical Report, Automation Technology Laboratory, Helsinki University of Technology, 1996.
- 3 Halme, A., Schönberg, T. and Wang, Y. Motion control of a spherical mobile robot. In 4th IEEE International

- Workshop on *Advanced Motion Control (AMC'96)*, Mie University, Japan, 1996.
- 4** **Koshiyama, A.** and **Yamafuji, K.** Design and control of an all-direction steering type mobile robot. *Int. J. Robotics Res.*, 1993, **12**(5), 411–419.
- 5** **Marigo, A.** and **Bicchi, A.** Rolling bodies with regular surface: controllability theory and application. *IEEE Trans. Autom. Control*, September 2000, **45**(9).
- 6** **Li, Z.** and **Canny, J.** Motion of two rigid bodies with rolling constraint. *IEEE Trans. Robotics and Automn*, 1990, **6**(1).
- 7** **Brockett, R.** and **Dai, L.** Nonholonomic kinematics and the role of elliptic functions in constructive controllability. In *Nonholonomic Motion Planning* (Eds Z. Li and J. F. Canny), 1993 (Norwell, Massachusetts and Kluwer, Dordrecht, The Netherlands).
- 8** **Jurdjevic, V.** The geometry of the plate-ball problem. *Arch. Rational Mechanics and Analysis*, 1993, **124**.
- 9** **Mukherjeen, R.** and **Das, T.** Feedback stabilization of a spherical mobile robot. In Proceedings of International Conference on *Intelligent Robots and Systems (IROS 2002)*, Lausanne, Switzerland, October 2002.
- 10** **Ashenden, P. J.** *VHDL Cookbook*, 1st edition, 1990 (Department of Computer Science, University of Adelaide, Australia).
- 11** **Craig, J. J.** *Introduction to Robotics: Mechanics and Control*, 2nd edition, 1989 (Addison-Wesley, Reading, Massachusetts).
- 12** **Paul, R. P.** *Robot Manipulators: Mathematics, Programming, and Control*, 1981 (The MIT Press, Boston, Massachusetts).
- 13** Low-power, 8-channel, serial 12-bit ADCs MAX186/MAX188. Datasheet from the ADC used, Maxim Integrated Products, 1996.
- 14** **Kanayama, Y. J.** and **Fahroo, F.** A new line tracking method for nonholonomic vehicles. In Proceedings of IEEE International Conference on *Robotics and Automation*, 1997, **4**, 2908–2911.
- 15** **Au, K. W.** and **Xu, Y.** Path following of a single wheel robot. In Proceedings of IEEE International Conference on *Robotics and Automation*, San Francisco, California, April 2000, pp. 2925–2930.
- 16** **Kolmanovsky, I.** and **McClamroch, N.** Developments in nonholonomic control problems. *IEEE Control Systems*, 1995, 20–36.